

Hidden charm pentaquark states and $\Sigma_c^{(*)}\bar{D}^{(*)}$ interaction in chiral perturbation theory

Lu Meng*, Bo Wang, Guang-Juan Wang and Shi-Lin Zhu

*School of Physics and State Key Laboratory of Nuclear Physics and Technology,
Peking University, Beijing 100871, China*

**E-mail: lmeng@pku.edu.cn*

We adopt the chiral perturbation theory to calculate the $\Sigma_c^{(*)}\bar{D}^{(*)}$ interaction to the next-to-leading order (NLO) and include the couple-channel effect in the loop diagrams. We reproduce the three P_c states in the molecular picture after including the $\Lambda_c\bar{D}^{(*)}$ intermediate states. We also discuss some novel observations arising from the loop diagrams.

Keywords: Pentaquark states; Chiral perturbation theory; Molecular states.

1. Introduction

In 2015, the LHCb Collaboration discovered two pentaquark candidates $P_c(4380)$ and $P_c(4450)$ in the $J/\psi p$ invariant mass spectrum of $\Lambda_b \rightarrow J/\psi K p$ ¹ (or see Ref. 2 for a review). Recently, the LHCb Collaboration updated these results³. The previously reported $P_c(4450)$ was resolved into two states $P_c(4440)$ and $P_c(4457)$, and a new state $P_c(4312)$ was observed with 7.3σ significance. These three states are narrow and their masses lie below the thresholds of $\Sigma_c\bar{D}^{(*)}$. Thus, they are good candidates of the $\Sigma_c\bar{D}^{(*)}$ molecules. The theoretical calculation in different approaches all supports their molecular nature⁴⁻⁷.

Chiral perturbation theory (ChPT) is the effective field theory of low energy QCD, which was used to build the modern theory of nuclear force^{8,9}. In this work, we adopt the ChPT to study the $\Sigma_c^{(*)}\bar{D}^{(*)}$ interaction^{10,11}, which is less model-dependent than other previous works. We take the loop diagrams into consideration, which give rise to some novel effects.

2. Formalism

The ChPT is performed to calculate the $\Sigma_c^{(*)}\bar{D}^{(*)}$ effective potentials to the next-to-leading order (NLO). The topological diagrams involved in the

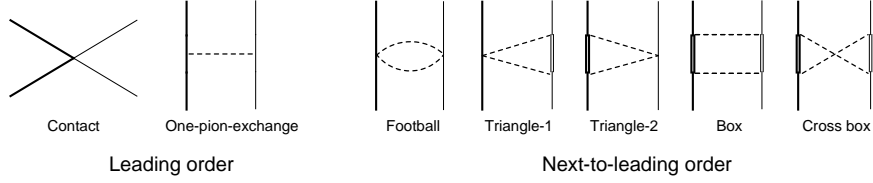


Fig. 1. Topological diagrams contributing to the LO and NLO $\Sigma_c^{(*)} \bar{D}^*$ interaction.

calculation are presented in Fig. 1. The leading order (LO) diagrams include the tree level contact interaction and one-pion-exchange diagrams. The NLO diagrams are the two-pion-exchange ones. In our calculation, the intermediate matter fields (double lines in Fig. 1) could be Σ_c , Σ_c^* , \bar{D} and \bar{D}^* . We keep the mass splittings between the heavy quark spin (HQS) partner states, thus our results could give the heavy quark spin symmetry (HQSS) violation effect. Since the $\Sigma_c^{(*)} \Lambda_c \pi$ couplings are competitive compared with the $\Sigma_c^{(*)} \Sigma_c^{(*)} \pi$ ones, we also include the Λ_c as the intermediate states in the loops.

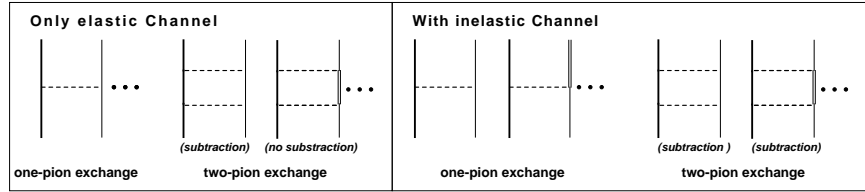


Fig. 2. Two approaches to couple-channel effect.

For the box diagrams, we could deal with the couple-channel effect through two approaches as illustrated in Fig. 2. From the view of time-ordered perturbation theory (TOPT), the box diagrams can be divided into the one-pion-iteration part and other part, see Fig. 3. For the one-pion-iteration part, the amplitude reads,

$$\mathcal{M} \sim (E_{\text{initial}} - E_{\text{inter}})^{-1} \approx \left[\left(m_1 + m_2 + \frac{\mathbf{p}_1^2}{2m_1} + \frac{\mathbf{p}_2^2}{2m_2} \right) - \left(m'_1 + m'_2 + \frac{\mathbf{p}'_1{}^2}{2m'_1} + \frac{\mathbf{p}'_2{}^2}{2m'_2} \right) \right]^{-1}. \quad (1)$$

When the intermediate states are the same as the external lines, i.e., $m_1 = m_2$ and $m'_1 = m'_2$, like NN systems, the amplitude would be am-

plified to destroy the power counting. We adopt the Weinberg's formalism to handle this problem¹². We subtract the one-pion-iteration part in the box diagrams and recover their contribution by solving the Lippmann-Schwinger or Schrödinger equation. For $\Sigma_c^{(*)}\bar{D}^{(*)}$ systems, the intermediate states could be different from the external lines. The power counting works well for these box diagrams. Therefore, we could either subtract the one-pion-iteration part and include inelastic channels in tree diagrams or keep the one-pion-iteration part and only include the elastic channels in tree diagrams. In this work, we adopt latter approaches as shown in the left panel of Fig. 2.

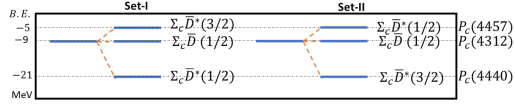
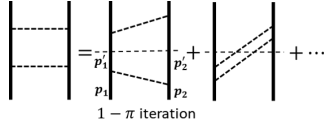


Fig. 3. Box diagrams in TOPT. Fig. 4. Two possible spin assignments for P_c states.

3. Results and discussions

Our LO results keep the heavy quark symmetry, which read,

$$\mathcal{V}_{\Sigma_c \bar{D}} = V_c, \quad \mathcal{V}_{\Sigma_c \bar{D}^*} = V_c + V_{ss} \mathbf{S}_1 \cdot \mathbf{S}_2. \quad (2)$$

There are two possible spin assignments for the three P_c states as shown in Fig. 4. Three states have the same central potential and their binding energy splittings arise from the spin-spin interaction. If we treat spin-spin interaction as a perturbation, the ratio of the binding energy splitting is exactly the ratio of spin-spin interaction. Therefore, the spin Set-I in Fig. 4 is favored.

At the NLO, we include loop diagrams which bring some novel effects. The mass splittings between HQS partner states give rise to considerable HQSS violation for $\Sigma_c^{(*)}\bar{D}$ systems. Meanwhile, the new spin structure $(\mathbf{S}_1 \cdot \mathbf{S}_2)^2$ appears at the loop level for the $\Sigma_c^* \bar{D}^*$ ¹¹, which is different from the two nucleon systems.

We have two unknown low energy constants (LECs), \mathbb{D}_1 and \mathbb{D}_2 , to the NLO. We vary the two LECs and try to reproduce three states simultaneously. The result is presented in Fig. 5. Three bands correspond to the regions of parameters in which the bound states have the binding energy

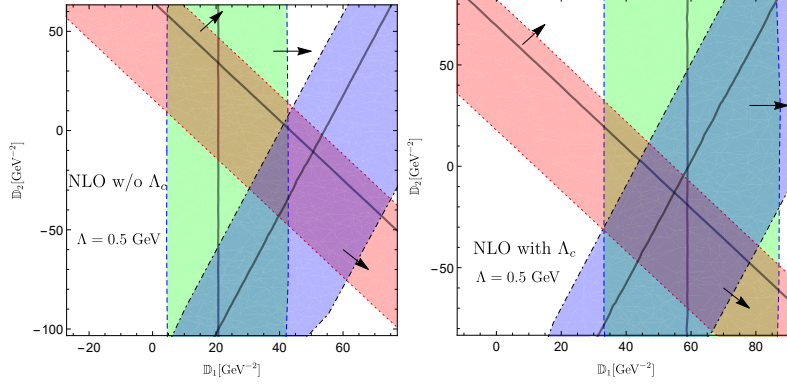


Fig. 5. The numerical results without and with Λ_c intermediate states to the NLO.

$[-30, 0]$ MeV. The three black lines represent the set of parameters corresponding to the experimental results. The left and right graphs in Fig. 5 are the results without and with the Λ_c as intermediate states, respectively. The three P_c states can coexist only when the couple-channel effect from $\Lambda_c \bar{D}^{(*)}$ is considered¹¹. With the \mathbb{D}_1 and \mathbb{D}_2 being fixed, there exist bound solutions for all seven S -wave $\Sigma_c^{(*)} \bar{D}$ channels as listed in Table. 1. It is possible to find the predicted states in the future experiments.

Table 1. The binding energies ΔE of $I = \frac{1}{2}$ hidden-charm $\Sigma_c^{(*)} \bar{D}^{(*)}$ systems.

	$[\Sigma_c \bar{D}]_{\frac{1}{2}}$	$[\Sigma_c \bar{D}^*]_{\frac{1}{2}}$	$[\Sigma_c \bar{D}^*]_{\frac{3}{2}}$	$[\Sigma_c^* \bar{D}]_{\frac{3}{2}}$	$[\Sigma_c^* \bar{D}^*]_{\frac{1}{2}}$	$[\Sigma_c^* \bar{D}^*]_{\frac{3}{2}}$	$[\Sigma_c^* \bar{D}^*]_{\frac{5}{2}}$
ΔE	-4.6	-22.5	-3.2	-34.5	-14.3	-3.4	-0.3

In Table 2, we compare the $\Sigma_c^{(*)} \bar{D}^{(*)}$ systems with two nucleon systems. $\Sigma_c^{(*)} \bar{D}^{(*)}$ interactions have some interesting features which do not appear in N - N systems. For example, the chiral dynamics for $\Sigma_c^{(*)} \bar{D}^{(*)}$ systems is the interplay between the light-light diquark in the charmed baryons and the light quark in the charmed mesons. Thus, one should take all the heavy quark partner states of charmed hadrons into consideration to include the whole interacting elements.

Our analytical results are pion mass dependent. The lattice QCD simulations for the $\Sigma_c^{(*)} \bar{D}^{(*)}$ systems are called for. Our expressions could be used to extrapolate the lattice QCD results to the physical pion mass¹³.

Table 2. Comparisons of the $\Sigma_c^{(*)}\bar{D}^{(*)}$ and N - N systems.

	N - N	$\Sigma_c^{(*)}\bar{D}^{(*)}$
Chiral dynamics	$N - N$	(light diquark)-(light quark)
Inter. states	Δ	Λ_c
Inter. states	-	HQS partner states e.g., $c(qq)_{s=1}^{I=1} = \Sigma_c + \Sigma_c^*$
Heavy quark limit	-	Pinch singularity in elastic channel Including inelastic channel
M_{inter} vs M_{initial}	$M_\Delta > M_N$	e.g., $M_{\Lambda_c} + M_\pi < M_{\Sigma_c}$
Imaginary part	w/o	w/
Small scale expansion	works	fails in $\Sigma_c\bar{D} - \Lambda_c\bar{D}^* - \Sigma_c\bar{D}$
Spin structure	$\sigma_1 \cdot \sigma_2$	$S_1 \cdot S_2, (S_1 \cdot S_2)^2 \dots$
Weinberg composite	$ E_D \ll \frac{m_\pi^2}{2\mu}$	$ E_{P_c} \sim \frac{m_\pi^2}{2\mu} \approx 9 \text{ MeV}$

ACKNOWLEDGMENTS

This project is supported by the National Natural Science Foundation of China under Grants 11575008, 11621131001.

References

1. LHCb Collab. (R. Aaij *et al.*), *Phys. Rev. Lett.* **115**, 072001 (2015).
2. H. X. Chen, W. Chen, X. Liu and S. L. Zhu, *Phys. Rept.* **639**, 1 (2016)
3. LHCb Collab. (R. Aaij *et al.*), *Phys. Rev. Lett.* **122**, 222001 (2019).
4. R.Chen, Z.F.Sun, X.Liu and S.L.Zhu, *Phys. Rev. D* **100**, 011502 (2019).
5. M. Z. Liu, Y. W. Pan, F. Z. Peng, M. Sánchez Sánchez, L. S. Geng, A. Hosaka and M. Pavon Valderrama, *Phys. Rev. Lett.* **122**, 242001 (2019).
6. F. K. Guo, H. J. Jing, U. G. Meißner and S. Sakai, *Phys. Rev. D* **99**, 091501 (2019).
7. M. L. Du, V. Baru, F. K. Guo, C. Hanhart, U. G. Meißner, J. A. Oller and Q. Wang, arXiv:1910.11846.
8. E. Epelbaum, H. W. Hammer and U. G. Meißner, *Rev. Mod. Phys.* **81**, 1773 (2009).
9. R. Machleidt and D. R. Entem, *Phys. Rept.* **503**, 1 (2011).
10. L. Meng, B. Wang, G. J. Wang and S. L. Zhu, *Phys. Rev. D* **100**, 014031 (2019).
11. B. Wang, L. Meng and S. L. Zhu, arXiv:1909.13054.
12. S. Weinberg, *Nucl. Phys. B* **363**, 3 (1991).
13. Z. W. Liu, J. M. M. Hall, D. B. Leinweber, A. W. Thomas and J. J. Wu, *Phys. Rev. D* **95**, 014506 (2017)